Journal of Physics: Conference Series **609** (2015) 012008 doi:10.1088/1742-6596/609/1/012008

Strain effects on effective masses for MoS_2 monolayers

E. R. Ortiz[1], Blanca Biel[1], Luca Donetti[1], Andrés Godoy[1], Francisco Gámiz[1]
[1]Dpto. Electrónica y Tecnología de Computadores, Facultad de Ciencias, Campus de Fuente Nueva, & CITIC, Campos de Aynadamar, 18071 Universidad de Granada, Spain

E-mail: biel@ugr.es

Abstract: We have studied the effects of both intrinsic and external factors, such as strain, substrate and electric field, over a MoS_2 monolayer, via DFT simulations. From these simulations we computed the system's bandstructure and evaluate the bandgap values, extracting the effective masses as well. Our calculations show a transition between direct and indirect gaps when strain is applied, and also that the bandstructure is barely affected by the presence of a substrate or an external electric field with values up to 1 V/Å .

1. Introduction

In recent years, two-dimensional (2D) materials, such as graphene, have drawn great attention for their possible applications in nanoelectronics. As the name implies, these materials are formed by a single atomic or molecular layer, with different layers stacking together under the effect of the so called van der Waals forces, which can be used to create complex heterostructures [1-3] while keeping the side effects of coupling different materials at a minimum.

One of those materials is molybdenum bisulfide (MoS_2), where the main monolayer is formed by three sublayers, as shown in Fig. 1. MoS_2, unlike graphene, behaves as a semiconductor with indirect gap (bulk) or direct gap at the K point (monolayer) [4-6], which may prove useful for the design of nanoelectronic devices.

Therefore, tuning these properties is essential if MoS_2 is to be implemented in future nanoelectronic devices. In this work, we study the effect on the bandstructure and effective masses of both structural changes, via straining, or external, in the form of a perpendicular electric field or a silicon oxide substrate.

2. Methodology

All the DFT calculations have been performed using SIESTA [7], within the Generalized Gradient Approximation (GGA) and the pseudopotential approaches.

Content from this work may be used under the terms of the Creative Commons Attribution 3.0 licence. Any further distribution of this work must maintain attribution to the author(s) and the title of the work, journal citation and DOI.
Published under licence by IOP Publishing Ltd

We have used the SIMPLEX algorithm [8] to optimize the DZP basis set for monolayer MoS_2 and SiO_2, in their experimental lattice constants of 3.160 Å and 4.914 Å, respectively. This lattice constant corresponds to the silanol reconstruction of crystalline α-quartz, which has been widely used in previous works [9, 10].

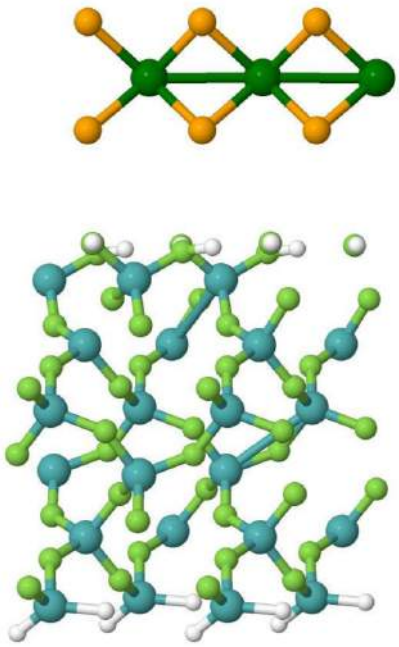

Figure 1. Top: side view of the MoS_2 monolayer. Sulfur is marked as orange (light) atoms, while molybdenum is represented as a green (dark) atom. 3 unit cells are represented.
Bottom: silanol substrate. Silicon atoms are represented on blue (dark) and oxygen as green (light). The white atoms on the surfaces represent the hydrogen atoms.

To accomplish with the 3D periodicity in SIESTA, a 2D monolayer requires a manual separation on the perpendicular z axis, 20 Å in this case, to avoid interaction between different layers. This also affects the Brillouin zone sampling, where we used a Monkhorst-Pack scheme of 9x9x1 points. We relaxed the structure until atomic forces were bellow 0.01 eV/ Å. The obtained bandgap value for unstrained MoS_2 is 1.81 eV, close (albet accidentally [11-13]) to the experimental 1.8 eV [4-6].

After the first monolayer simulation, we performed several strain tests using strain values of 3.66% and -3%, applied on both *x* and *y* axes. The first value corresponds to the expected strain caused by an α-quartz substrate as described above. These simulations were later repeated, adding an external electric field of 0.25, 0.5 and 1 eV/ Å and a silanol substrate.

In all these cases we also calculated the effective masses on both valence and conduction bands, using a parabolic approach to obtain the band curvature at the special points in the reciprocal space.

3. Results

3.1. Strain effects on the bandstructure.

In previous sections, we introduced bulk MoS_2 as an indirect gap semiconductor, while unstrained, monolayer MoS_2 behaves as a direct gap semiconductor with a 1.8 eV gap. However, once the biaxial strain has been applied, the gap becomes indirect once again, as shown in Fig. 2. Fig. 2 contains four calculated bandstructures along the $\bar{\Gamma}$-M-K-$\bar{\Gamma}$ path of the Brillouin zone, for unstrained MoS_2, compressive and tensile strain. For compressive strain, our simulations show a displacement of the conduction band minimum (CBM) from the original K point to a midpoint between the K and $\bar{\Gamma}$

points, resulting on an indirect gap, as already reported on previous works[14, 15]. For tensile strain, in both cases the valence band maximum (VBM) switches from the K point to the $\bar{\Gamma}$ point, leading to another indirect bandgap. For all the studied strain values, the value of the direct bandgap at the K point decreases, from a maximum of 2.16 eV while compressed to a minimum of 1.44 while tensed at the maximum strain considered on this work. Fig. 3 shows a more detailed description, including other possible transitions.

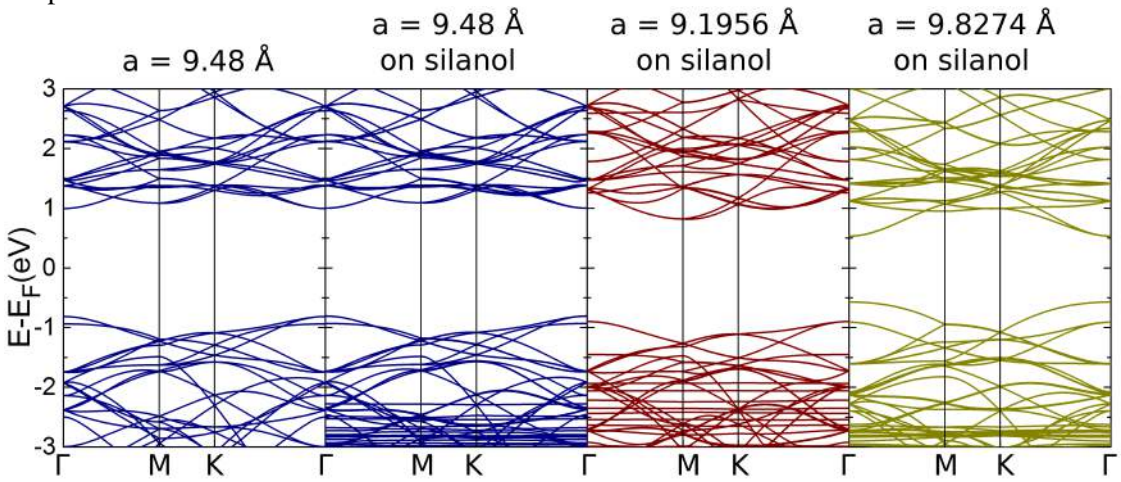

Figure 2. Monolayer MoS_2 bandstructure for different strains. From left to right: isolated, unstrained monolayer; unstrained, tensely and compressively strained on a silanol substrate. To match sizes with the substrate a 3x3 supercell was used to recreate the MoS_2 layer.

3.2. Effective masses.

To calculate the effective masses, we fitted the extremes of the obtained bandstructures at the relevant symmetry points of the Brillouin zone. Our results are summarized in Fig. 3, which contains the different values for electron and holes mass in all of those points, for all the different strains. In particular, the results obtained for hole mass in the unstrained sample are in good agreement with the literature, with m^*/m_0=0.67 for the K point and m^*/m_0=3.34 for the $\bar{\Gamma}$ point, versus the m^*/m_0=0.64 and m^*/m_0=3.52 from previous works[14].

3.3. SiO_2 substrate and external electric field

In order to study the effects of external factors, we set an external electric field on the perpendicular direction of the 2D layer, with values ranging from 0.25 V/Å to 1V/Å, for all the different afore mentioned strain values. For all these cases, the field does not induce appreciable modifications on the bandstructure.

As for the silanol substrate, our results match once again those proposed in the literature [16], showing that the presence of a substrate does not affect the bandstructure enough to cause a change the effective masses, which remain the same as in the previous sections but for the presence of the oxide bands for energies far form the Fermi level. In Figure 2, the bandstructures for different strain values are shown, with and without the presence of the substrate, for comparison. Other than the change caused from the increased supercell, the states created by silanol remain away from the bandgap, causing no remarkable changes.

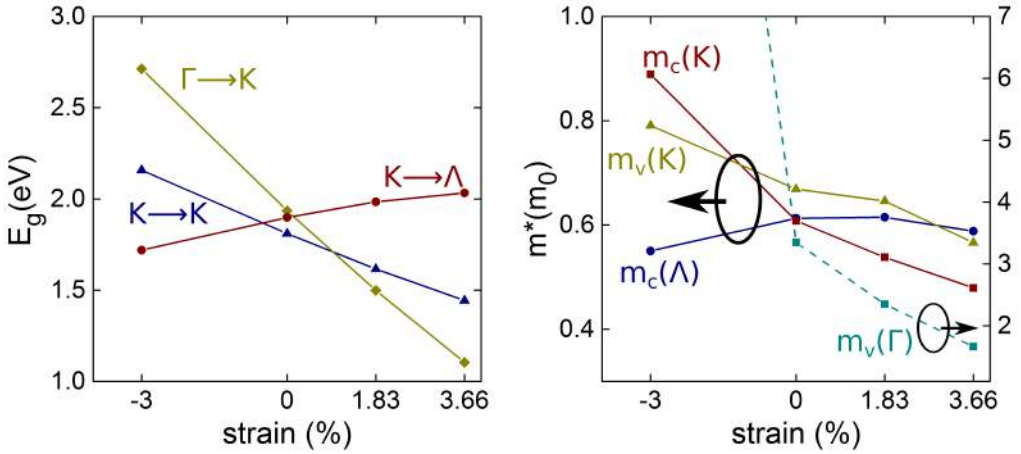

Figure 3. Left panel: bandgap values for the transitions between VBM and CBM at the relevant points of the Brilloun zone. Right panel: effective masses for holes and electrons on each relevant point of the Brillouin zone for the studied strain values.

4. Conclusions

We calculated the bandstructure for MoS_2 under different strain effects, external electric fields and on a silanol substrate. From such bandstructures the effective masses were calculated for the relevant symmetry points of the Brillouin zone. Strain simulations show a transition from direct to indirect gap, while neither the electric field nor the silanol substrate barely affect the bandstructure.

5. Acknowledgements

B. Biel thankfully acknowledges funding by the RYC-2012-10381 contract from Ramón y Cajal Program (MINECO) and computer facilities provided by the RES-BSC and the CSIRC-UGR supercomputing centers. A. Godoy acknowledges funding by the MINECO contract FIS 2011-26005.

6. References

[1] A. K. Geim and I. V. Grigorieva, Nature 499 (2013), 419
[2] A. Hsu et al., Proceedings of the IEEE 101 (2013), 1638
[3] G. Fiori et al. Nature Nanotechnol. 9 (2014), 768
[4] K. F. Mak, et al., Phys. Rev. Lett. 105 (2010), 136805
[5] A. Splendiani et al., Nano Lett. 10 (2010), 1271
[6] A. Kumar and P. K. Ahluwalia, Eur. Phys. J. B 85 (2012), 186
[7] J.M. Soler et al., J. Phys.: Condens. Matter 14 (2002), 2745
[8] W. Press et al., Numerical Recipes, Cambridge U. Press, (1989)
[9] M.H. Evans et al. Phys. Rev. Lett. 95 (2005), 106802
[10] T. Hara et al., J. Phys. Conf. Ser. 109 (2008), 012012
[11] K. Dolui et al. Phys. Rev. B 85 (2012) 205302
[12] A. Ramasubramaniam, Phys. Rev. B 86 (2012) 115409
[13] T. Cheiwchanchamnangij and W. R. L. Lambrecht, Phys. Rev. B 85 (2012) 205302
[14] W. S. Yun et al., Phys. Rev. B 85 (2012), 033305
[15] N. Harada et al., J. Appl. Phys. 115 (2014), 034505
[16] K. Dolui et al., Phys. Rev. B 87 (2013), 16540